1 OPY PAPER

Microwave signatures of melting/refreezing snow: observations and modeling using dense medium radiative transfer theory

Marco Tedesco, Edward J Kim
Anthony England, Roger de Roo,
Janet Hardy

Abstract

Introduction

Snow is a fundament element of the Earth's hydrologic and energy cycles influencing the land surface albedo and the net radiation balance. It covers more than the half of the Northern hemisphere land surface (around 60 %) in mid winter and over 30% of Earth's total land surface is covered by seasonal snow [Robinson, et al., 1993]. At high latitudes and altitudes, where snowfall is the dominant type of precipitation [Serreze et al., 2000], melting snow is responsible for most of the total annual streamflow. Climatologically, when snow melts, the increase in the amount of liquid water in the snowpack increases the albedo with consequent effects on the influence of snow on the radiation balance.

Microwaves are sensitive to snow properties and several techniques have been proposed in the literature for the retrieval of snow parameters from satellite remotely sensed data [i.e. Goodison and Walker, 1993; Chang, et al., 1996; Shi and Dozier, 2000, Tedesco, Chang, Hallikainen]. While visible and near-infrared sensors cannot see through clouds and without an adequate solar illumination, measurements in the microwave spectral regions can be largely insensitive to weather conditions and they do not require solar illumination. Besides, the microwave signal provides information on the internal

properties of the snowpack (i.e. such as snow water equivalent), where visible and infra-red sensors cannot.

Microwave emission of snow is sensitive to the phase of water, mean grain size, fractional volume and snow depth. In dry snow, which can be represented as ice particles embedded in an air background, the mechanism dominating the microwave signal is the volumetric scattering due to the scatterers (ice particles). In wet snow, when water is also present in liquid phase, the snowpack can be modeled as a mixture of ice, water and air. The absorption coefficient is higher than that one of the dry snow as a consequence of the increase of the imaginary part of the effective permittivity.

Microwave brightness temperatures of snow covered terrains can be modeled by means of the Dense Radiative Transfer Medium Theory (DMRT) [Tsang aet al. 1985, 2000, Jin]. In a dense medium, such as snow, the assumption of independent scattering is no longer valid and the scattering of correlated scatterers must be considered. In the DMRT, this is done considering a pair distribution function of the particles position. In the electromagnetic model, the snowpack is simulated as a homogeneous layer having effective permittivity and albedo calculated through the DMRT. In order, to account for clustering of snow crystals, a model of cohesive particles can be applied [Zurk], where the cohesion between the particles is described by means of a dimensionless parameters called *stickiness* (τ), representing a measure of the inversion of the attraction of the particles. The lower the τ the higher the stickiness.

In this study, microwave signatures of melting and refreezing cycles of seasonal snowpacks at high altitudes are studied by means of both experimental and modeling tools. Radiometric data were collected 24 hours per day by the University of Michigan Tower Mounted Radiometer System (TMRS) during the Fourth Intensive Observation Period (25-30 March 2003, IOP4) of the Cold Land Processes Experiment-1 (CLPX-1) at the Local Observation Scale Site (LSOS). The LSOS was located in the Fraser experimental forest (Colorado) and represented the smallest of the test sites selected for the CLPX. Meteorological measurements of snow and soil parameters were recorded 24 hours per day by means of the University of Michigan meteorological station and snow pit measurements were carried out at locations close to the area observed by the radiometer. The brightness temperatures collected by means of the TMRS are simulated by means of a multi-layer electromagnetic model based on the dense medium theory with the inputs to the model derived from the data collected at the snow pits and from the meteorological station.

The paper is structured as follows: in the first Section the temperature profiles recorded by the meteorological station and the snow pit data are presented and analyzed; in the second Section, the characteristics of the radiometric system used to collect the brightness temperatures are reported together with the temporal behavior of the recorded brightness temperatures; in the successive Section the multi-layer DMRT-based electromagnetic model is described; in the fourth Section the comparison between modeled and measured brightness temperatures is discussed. We dedicate the last Section to the conclusions and future works.

I. Measurement of snow properties

Temporal trends of temperature profiles

The temporal trends of the snow and air temperatures were recorded 24 hours per day by means of the University of Michigan meteorological station using 14 probes at fixed heights above the ground surface (152.4 cm, 143.0 cm, 131.3 cm, 119.6 cm, 107.9 cm, 96.2 cm, 84.5 cm, 72.8 cm, 61.1 cm, 49.4 cm, 37.7 cm, 26.0 cm, 14.2 cm and 2.5 cm). Obtained results are plotted in Figure 1. In particular, Figure 1 (a) shows the temporal behaviour of the temperatures collected between 154 and 84.5 cm above the ground surface, Figure 1 (b) plots the temporal behaviour of the temperatures recorded between 84.5 to 61 cm and, finally, Figure 1 (c) reports the temporal behaviour of the temperatures recorded between 48.5 cm and the ground surface. As the thermometers were kept fixed with respect to the ground surface, they measured the snow or air temperature, depending on the snow depth. The probes between 154 and 72.8 cm measured air temperature for the entire IOP4. The probes between 61.1 cm and the ground surface were covered by snow. From the collected data we observe that in the period between March 25 2004 00:00 (local time) and March 27 2004 12:00 (corresponding to 60 hours from the reference time, being March 25, 00:00), the temperature of the upper part of the snow is oscillating around 0 ° C with the air temperature ranging between -15 ° C and + 6 ° C (Figure 1 (b)). The temperature of the bottom part of the snowpack is always slightly higher than zero (around 0.5 ° C) and stable (Figure 1 (c)). As a consequence, the bottom part of the snowpack was wet for the entire IOP4. The upper part of the snowpack was subject to melting and refreezing

cycles. In the period between March 27, 2004 (72 hours from the reference time) and the end of the IOP4, a change in the trend of the temperatures recorded at 49.5 and 37.7 cm is well observable. This could be due to the strong decrease of the air temperature and to presence of new fresh snow.

Snow pit measurements

Snow depth, density, temperature, wetness and mean grain size along were collected along the vertical profile at different locations of the LSOS [**18**]. Two of these locations (# 3 and # 4) were close to the snow monitored by the meteorological station and by the TMRS. The snow pits data used for our study were collected from snow pit location # 3 on March 26 2004 at 10:00 (3A), March 28 2004 at 16:50 (3B) and March 30 2004 at 16:00 (3C), where the data from the snow pit location # 4 were collected on March 25 2004 at 10:50 (4A), March 27 2004 at 11:45 (4B) and March 29 2004 at 14:30 (4C). Values of snow parameters averaged along the vertical profile are reported in Table 1, in Section V. As an example of measured profiles, Figure 2 shows the temporal trend of snow wetness profiles, with white color corresponding to dry snow, light gray to wetness lower than 0.5 %, medium gray to wetness between 0.5 and 1 %, dark gray to wetness between 1 and 1.5 % and, finally, black to wetness higher than 1.5 %. Figure 3 shows a picture of the snow pit where measurements were performed on March 29. In the picture, the dry snow layers overlying the wet ones are well observable. The measured profiles of snow wetness confirm that the bottom part of the snowpack was wet for the entire IOP4, as expected given the temperatures recorded by the meteorological station. With regard to the upper part of the snowpack, data collected on March 25, 2003 show that a dry snow

layer was overlying two layers of wet snow with different wetness which, in turn, were overlying another layer of dry snow over wet snow. On March 26, 2003 also the upper part of the snowpack is wet where on March 27, 2003 was almost dry (w = 0.06 %) and on March 28 and March 29, 2003 the upper part of the snowpack was again dry. On March 30, another dry snow layer between wet snow layers is observed.

II. The microwave radiometric system and data

During the IOP4 of the CLPX, several types of snow conditions were observed, from dry to wet snow through several cycles of melting and refreezing. Radiometric data at 6.8, 19 and 37 GHz (vertical and horizontal polarizations) were recorded 24 hours per day with a fixed incidence angle of 53 degrees by means of the University of Michigan Truck-Mounted Radiometer System (TMRS). The 19 and 37 GHz systems had beamwidths of 10° each while the 6.8 GHz system had beamwidths of 22°. The antennas were mounted on the end of a 10-meter telescoping boom with an elevation positioner at the end of the boom allowing incidence angle variation from nadir to zenith.

The temporal trends of the brightness temperatures (vertical polarization) recorded at 6.8 (dark grey), 19 (light grey) and 37 GHz (black) by the TMRS are plotted in Figure 4. Air and surface snow temperatures, represented by the temperatures recorded at 61.1 and 72.8 cm above the surface by the meteorological station, are also reported.

From the Figure we observe that two complete melting-refreezing cycles occurred within the first 36 hours of the IOP4 (reference time is March 25, 00:00). At 37 GHz the changes in the brightness temperatures due to the melting-refreezing cycles are stronger than those at 19 GHz. This can be explained considering that the highest frequency is more sensitive to the surface changes of the snowpack properties (i.e. temperature, wetness, grain size), where the melting or refreezing was occurring. At 6.8 GHz, the sensitivity to the melt-refreeze process is very weak, because of low sensitivity to volumetric scattering and of the high penetration depth. Recorded brightness

temperatures can be explained considering that during the melting and refreezing cycles the liquid water content (LWC) is strongly responsible for the behaviour of the brightness temperatures during the melting and refreezing cycles. For dry snow (LWC = 0), volumetric scattering is dominant on absorption and, in first approximation, the brightness temperature can be modelled as the brightness temperature of the soil reduced by the scattering of dry snow particles plus the brightness temperature of the snow itself. When snow melts (LWC > 0), the imaginary part of the permittivity of snow increases and so does the absorption coefficient. The brightness temperatures increase as the wetness increases until a saturation value is reached. After this, the brightness temperatures remain constant as the wetness increases. During the refreezing, the brightness temperatures decrease as the LWC and temperature in the snowpack decrease. It is important here to point out that when snow is dry the total brightness temperature is mainly due to the brightness temperature of the soil reduced by the scattering from dry snow particles. When snow is wet, the radiation emitted by the soil is absorbed by snow and the main contribution to the recorded brightness temperature is due to the upper part of the snow pack.

No melting cycle occurs in the period between March 26 2004 at 12:00 and March 29 2004 at 10:00 (60 and 130 hours on the graph). In this period, the recorded brightness temperatures decrease, reaching the minimum on March 27 2004 at 4:00 (100 hours) either because of the decrease of the snow temperature (as already observed in Figure 1 (c) the snow temperature in this period at different heights is always below zero) and because of the increase of the mean particle size.

After this period, new melting-refreezing cycles are observed until the end of the IOP4.

The temporal trend of the polarization index (PI=(V-H/V+H)*100)) at 37 GHz is reported in Figure 5 where the brightness temperature at 37 GHz at vertical polarization is also reported as a reference. In general, the polarization index decreases when snow melts and increases when snow freezes. This trend can be explained considering that when snow is dry, the vertical and horizontal polarizations are separated as a consequence of the volumetric scattering due to the ice particles. When snow melts, the presence of liquid water and roughness effects reduce the value of the polarization index.

IV. The electromagnetic model

In this Section, a multi-layer electromagnetic model based on Dense Medium Theory (DMRT) under the Quasi Crystalline Approximation with Coherent Potential (QCA-CP) ([3][4, 5, 7]) is proposed to simulate the brightness temperatures recorded by the TMRS. The use of DMRT is fundamental to describe propagation and scattering in snow, where the classical radiative transfer theory (CRT) fails and it is necessary to take into account for scattering of correlated particles through the ice particles distribution. In the model, the snowpack is divided into n layers and each of them is treated as a slab of distributed spherical particles with radius a, thickness d, wetness w (expressed in percentage on the total volume), total fractional volume f (given by the density of snow divided by the density of ice - ρ_{snow}/ρ_{ice}) and permittivity ε_i, embedded in a background medium of permittivity ε_b (Figure 6). For each layer, the total fractional volume is expressed by $f=f_{ice}+w/100$, where f_{ice} represents the fractional volume occupied by the ice particles and

w is the snow wetness.

We model snow wetness considering ice particles surrounded by a thin film of water. The effective dielectric constant of ice spheres with water coating is given by the solution of the following Eq. 1 [19]:

$$\frac{\varepsilon_{ws}-\varepsilon_0}{\varepsilon_{ws}+\varepsilon_0}=\frac{(\varepsilon_w-\varepsilon_0)(\varepsilon_i+\varepsilon_w)+S(\varepsilon_i-\varepsilon_w)(\varepsilon_0+2\varepsilon_w)}{(\varepsilon_w+2\varepsilon_0)(\varepsilon_i+2\varepsilon_w)+2S(\varepsilon_w-\varepsilon_0)(\varepsilon_i-\varepsilon_w)} \qquad \text{Eq. 1}$$

where ε_{ws} is the effective permittivity of the water-coated ice spherical particles, ε_w is the water permittivity, ε_i is the ice permittivity and $S = a_{ice}/a_{water}$, being a_{ice} and a_{water} the inner (only the ice particles) and outer (ice particles plus water film) radii of the coating sphere. The inner and outer radii may be related and the parameter S can be given by : $S = (f_{ice}/f_{tot})$ [3]. The model has an ulterior parameter, the *stickiness* (τ), which describes the fact that ice particles in nature tend to bond together to form aggregates. The stickiness describes the adhesion force between particles allowed to adhere together, with τ so that the smaller the τ the more sticky the particles [5, Zurk]. However, in this study we do not make use of the stickiness parameter. The reason lies in the fact that, although the parameter is justified by the physical behaviors of snow particles, it is still difficult to measure and quantify the stickiness from snow pit or ground observations. The selection of an appropriate value is difficult also in view of the high sensitivity of brightness temperatures to this parameter.

The final DMRT equations assume a form resembling the conventional radiative transfer theory and can be solved by using discrete ordinate form, the Gaussian quadrature and the eigen-values and eigen-vectors methods [3]. The unknown coefficients used to derive the particular solution from the eigen-vector solutions are determined by imposing the

boundary conditions. For example, in the case of $n = 3$ we have: $\bar{I}_1(\pi-\theta,0) = \bar{\bar{R}}_{10} \cdot \bar{I}_1(\theta,0)$ at $z = 0$, at $z = -d1$ $(d2)$, being $d1$ and $d2$ the thickness of the first two layers, $\bar{I}_1(\theta,-d1) = \bar{I}_2(\theta,-d1)$ $(\bar{I}_1(\theta,-d2) = \bar{I}_2(\theta,-d3))$ and $\bar{I}_2(\pi-\theta,-d1) = \bar{I}_2(\pi-\theta,-d1)$ $(\bar{I}_2(\pi-\theta,-d2) = \bar{I}_2(\pi-\theta,-d2))$, and at $z = -d3$ (snow/soil interface), $\bar{I}_2(\theta,-d3) = \bar{\bar{R}}_{3soil} \cdot \bar{I}_2(\pi-\theta,-d3) + \bar{\bar{T}}_{3soil} \cdot C \cdot T_{soil}$ with $R_\alpha(\theta) = [(1-Q)r_\alpha(\theta) + Qr_\beta(\theta)]\exp(-H \cdot \cos^2\theta)$. Q and H represent the parameters of the so called *Q/H* model [20] used to model the roughness at the soil/snow interface. The value of Q can be determined by differences between vertical and horizontal polarizations. The parameter *H* affects absolute measurements of brightness temperatures and it has been obtained from brightness temperatures when snowpack was thin (H = 0.2). The value of *Q* is chosen as 0.35 at 37 GHz and 0.4 at 19 GHz [Tsang, 2004].

V. Modeling of experimental data: results and discussion

In this Section, the brightness temperatures are simulated by means of the DMRT model using the snow parameters measured at the snow pits to derive the inputs to the electromagnetic model. The modeled brightness temperatures are, then, compared with those measured by the TMRS. The number of layers in which the snowpack is divided was kept fixed for the entire IOP4 and was initially fixed to $n = 3$. This value was initially suggested by the number if distinctive layers identified considering the wetness

and mean grain size distribution. However, because of the high wetness values of the bottom part of the snowpack, it is possible to reduce the number of layers to $n = 2$. Indeed, the penetration depth in wet snow at the frequencies and wetness of interest is lower than the thickness of the second layer of snow overlying that at the bottom. The thicknesses of the two layers changed depending on the snow wetness profile: the first layer was representative of the part of the snowpack subject to wetness ranging between 0 % and 4 % and the second (bottom) layer of a layer of wet snow with wetness between 0.5 % and 5 %.

In order, to obtain the inputs to the electromagnetic model the values of the snow parameters measured at the snow pits are vertically averaged. Table 1 reports the thickness, fractional volume, temperature and wetness for the considered dates. Note that in the case of wetness, when measured values of wetness of the upper part of the two layers in which the snowpack is divided was exceeding 0.5 %, only the last value was considered. Indeed, wetness measurements were carried out every 10 cm along the vertical profile and, according to [Maetzler], the penetration depth at the frequency f interest for values of wetness higher than that one considered is lower than 10 cm. Not considering this aspect during the derivation of the input parameters to the electromagnetic model can lead to underestimation or overestimation of the values of the brightness temperature. In example, if a layer of snow 10 cm thick with wetness 0.5 % is overlying another wet layer with wetness 1.8 % (0.1 %) , then the value of wetness to be considered is 0.5 % and not 1.15 % (0.3 %). The mean particle size is the parameter to which brightness temperatures are most sensitive, especially at 37 GHz. Profiles of the three classes of Small, Medium and Large particle size along the both short and long

directions were collected at the snow pit locations. Table 2 shows the weighted Averages of mean particle size using the values of the Small, Medium and Large classes (named case A), only the values of the Medium and Large (case B) or only the values of the class Large (case C).

In general, the values of brightness temperatures simulated in the case A are overestimated, especially in those cases when a dry snow layer is overlying a wet snow layer (snow pits 4A, 4B and 4C). The values of brightness temperatures simulated using the values computed in the case C are closer to the measured ones, but often underestimated.

The brightness temperatures simulated with the values obtained in the case B are reported in Figure 7. Squares represent the measured brightness temperatures where circles represent the simulated ones. Black symbols refer to vertical polarization where white symbols refer to horizontal polarization. Vertical bars on the simulated brightness temperatures represent the values of brightness temperatures when the mean grain size (diameter) ranges of ± 0.1 mm around the values used to plot the simulated values. The value of 0.1 mm is selected because the values of measured grain size are rounded to the nearest value, multiple of 0.1. ERROR

Conclusions

Microwave brightness temperatures of melting/refreezing cycles of snow recorded 24 hours per day during the IOP4 of the CLPX-1 have been analyzed. The observed behaviour of the radiometric quantities has been related to the melting and refreezing cycles of the observed snowpack. Snow pit data and temporal trend of temperature profiles recorded in conjunction with electromagnetic signatures have been also reported and discussed. A multi-layer electromagnetic model based on the Dense Medium Theory has been developed and implemented to simulate the brightness temperatures of both wet and dry snow. In the model, wet snow is treated as a mixture of ice particles surrounded by a film of water embedded in a background medium. Although the model included the possibility of using the stickiness parameter, we decided not to use this parameter because of the lack of measurements and information regarding this parameter. The measured brightness temperatures have been modelled using the values of snow parameters derived from snow field measurements as input to the electromagnetic model. Obtained results show that measured brightness temperatures can be modelled with a good accuracy using the snow parameters collected from the ground measurements. In particular, results suggest that the best matches between modelled and measured brightness temperatures can be achieved by averaging the only values of the Medium and Large classes, instead of including also the values of the Small class. When the last values are included, the model tends to overestimate the measured brightness

temperatures. Also, if only the values of the Large class are used the model tends to underestimate the recorded brightness temperatures.

Acknowledgment

References

[1 Marco Tedesco[1], Edward J. Kim[2], Don Cline[3], Tobias Graf[4], Toshio Koike[4], Janet Hardy[5] , Richard Armstrong and Mary Jo Brodzik,. Comparison of local-scale measured and modelled brightness temperatures and snow parameters from the Cold Land Processes Experiment 2003 by means of a dense medium theory model, submitted to Geoscience and Remote Sensing Letters, February 2003

[2 Tedesco, IEEE submitted

[3 Jin Y. Q., Electromagnetic scattering modelling for quantitative remote sensing, World Scientific, 1993

[4 L. Tsang , J. A. Kong and R. T. Shin, Theory of microwave remote sensing, Wiley-Interscience, 1985

[5 L. Tsang, C.T. Chen, A.T.C. Chang, J. Guo and K.H. Ding, Dense media radiative transfer theory based on quasicrystalline approximation with applications to passive microwave remote sensing of snow, Radio Science, 35, No. 3, May-June 2000, pp 731-749

[6 M. Tedesco, E. J. Kim, D. Cline, T. Graf, T. Koike, R. Armstrong, M. J. Brodzik and J.P. Hardy, "Modelling CLPX IOP3 Radiometric Data by Means of the Dense Media Theory: Preliminary Results for the LSOS Test Site" presented at American Geophysical Union Society, AGU Meeting, San Francisco, December 8-12 , 2003

[7 M. Tedesco, Microwave remote sensing of snow, PhD Thesis, Institute of Applied Physics 'Carrara', Italian National Research Council, IFAC – CNR, Microwave Remote Sensing Group, November 2003

[8 JOG, accepted

[9 Nelder, J. A. and R. Mead, A Simplex Method for Function Minimization, Computer Journal, Vol. 7, p. 308-313, 1965

[10 Convergence Properties of the Nelder--Mead Simplex Method in Low Dimensions, Jeffrey C. Lagarias, James A. Reeds, Margaret H. Wright, Paul E. Wright, SIAM Journal on Optimization , **Volume 9 , Issue 1 1998, Pages: 112 – 147, 1998 ISSN:1052-6234**

[11 G. Macelloni, S. Paloscia, P. Pampaloni and M. Tedesco, "Microwave Emission from Dry Snow: A Comparison of Experimental and Model Result," IEEE Trans. Geosci. Remote Sensing, vol. 39, n. 12, pp. 2649-2656, December 2001.

[12 IGARSS Ed kim

[13 S. Kazama, T. Rose, and R. Zimmerman. "A Precision Autocalibrating 7ch Radiometer for Environmental Research Applications" Journal of The Remote Sensing Society of Japan, Vol. 19, No. 3, pp. 37-45, 1999

[14 T. Graf, T. Koike, H. Fujii, M. Brodzik, and R. Armstrong. 2003. "CLPX-Ground: Ground Based Passive Microwave Radiometer (GBMR-7) Data". Boulder, CO: National Snow and Ice Data Center. Digital Media."

[15 Sihvola A., Electromagnetic mixing formulas and applications, IEE Electromagnetic Waves Series 47, England, 1999

[16 Hallikainen M.T>, Ulaby F. T., Abdelrazik M., Dielectric properties of snow in the 3 to 37 GHz range, IEEE Trans. On Antennas and Propagation, Vol. AP-34, No. 11, Nov. 1986, pp 1329-1339

[17 Hufford G., "A model for the complex permittivity of ice at frequencies below 1 THz",Int. Journ. Of Infrared and MM Waves, Vol. 12, No. 7 , 1991

[18 Hardy, J., J. Pomeroy, T. Link, D. Marks, D. Cline, K. Elder, R. Davis. 2003. Snow Measurements at the CLPX Local Scale Observation Site (LSOS). In situ data edited by M. Parsons and M.J. Brodzik. Boulder, CO: National Snow and Ice Data Center. Digital Media.

[19 Bohren C.F. and D.R. Huffman, Absorption and scattering of light by small particles, Wiley and Sons, New York, 1983

[20 J. R. Wang, P.E. O'Neill, T.J. Jackson and E. T. Engman, Multifrequency measurements of the effects of soil moisture, soil texture and surface roughness, IEEE Trans. Geosc. Remote Sensing, vol. 21, pp 4-51, Jan, 1983

[21 Shih S.-E., K.H. Ding, J. A. Kong and Y.E. Yang, Modeling of millimeter wave backscatter of time-varying snow cover, Progress in Electromagnetics Research, PIER 16, pp. 305-330, 1997

Figures and Tables

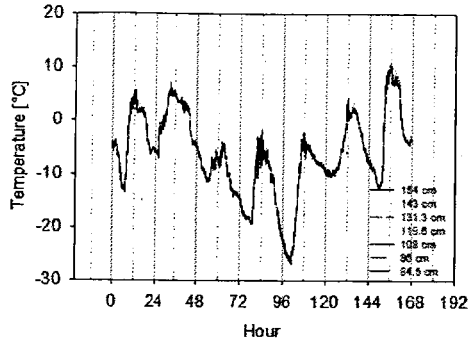

(a)

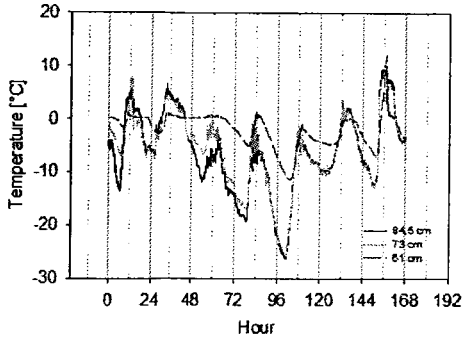

(b)

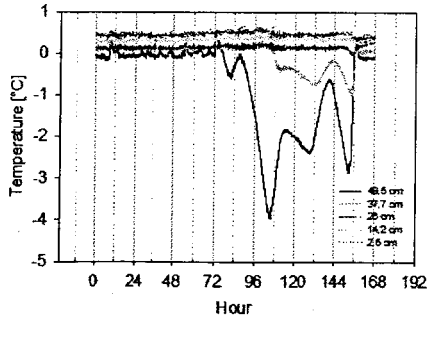

(c)

Figure 1

Temporal behaviours of temperatures profiles recorded by University of Michigan meteo station. Reference time is March 25, 00:00.

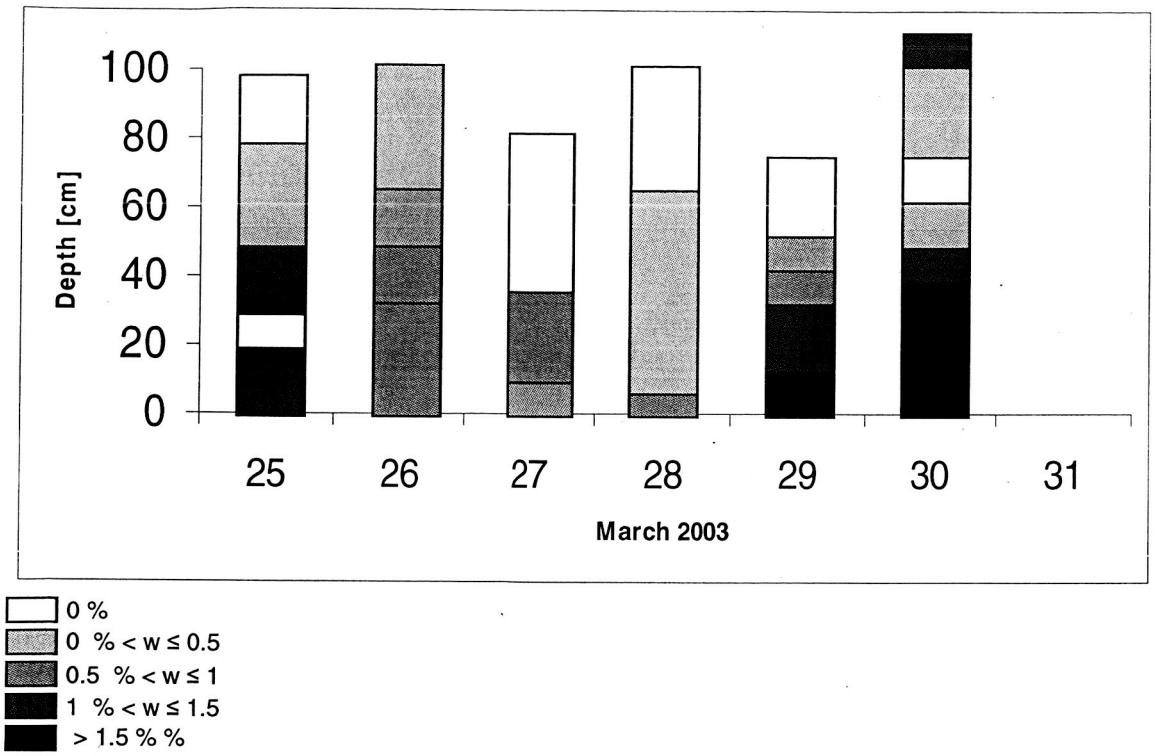

Figure 2

Snow wetness profiles collected at the snow pits # 3 (March 26,28 and 30, 2003) and # 4 (March 25,27 and 29, 2003). White → dry snow, light gray → 0 %< w < 0.5 %, medium gray 50 % → 0.5 % < w < 1 %, dark gray → 1 % < w < 1.5 %, black → w ≥1.5 %

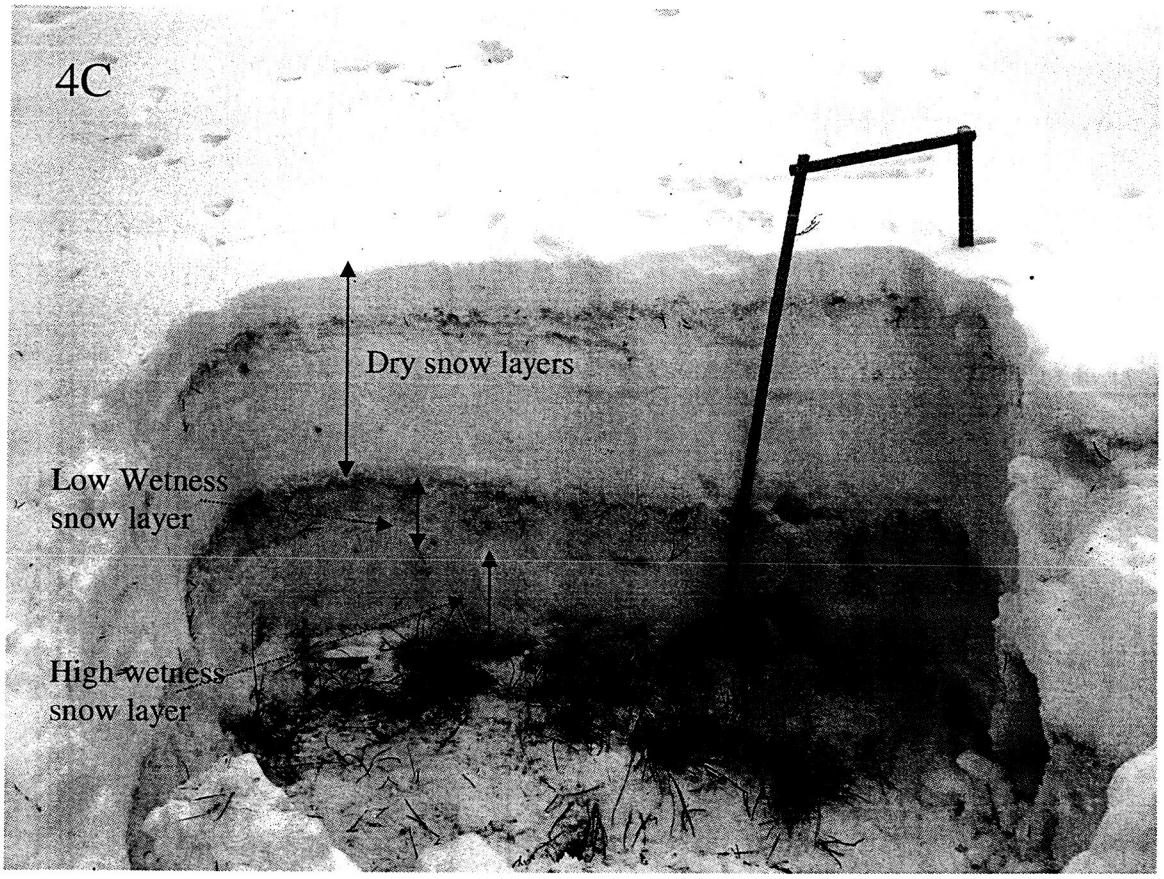

Figure 3

Photograph of the snow pit # 4 on March 29, 2003. The different types of observed layers are remarked.

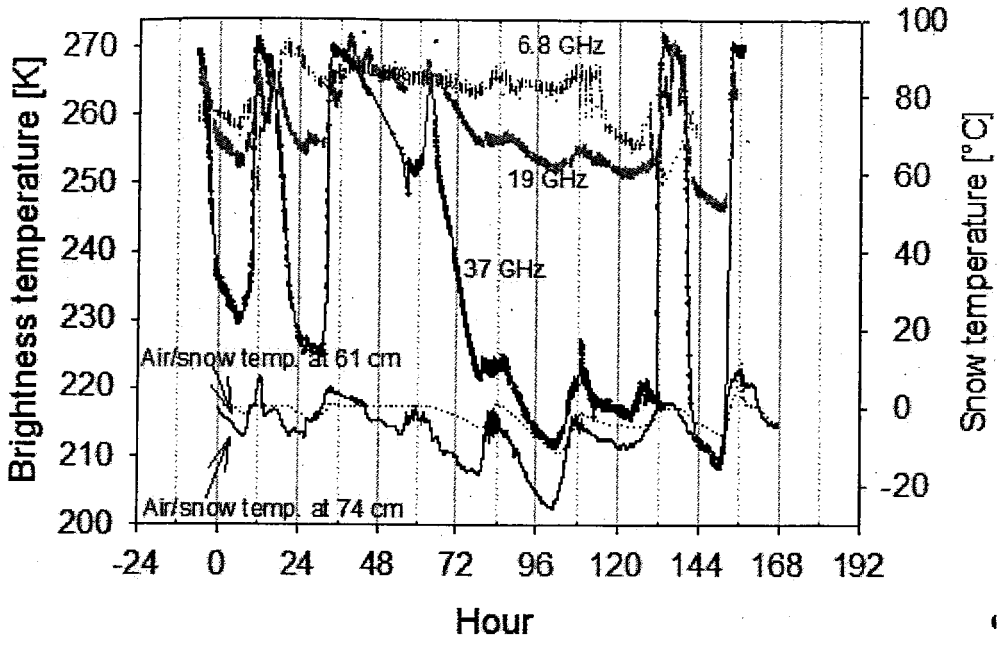

Figure 4 *Temporal trend of brightness temperatures at 6.8 (dark grey), 19(light grey) and 37 GHz (black) at vertical polarization measured by the UMTBMR as a function of time together with air/snow temperatures recorded at 61 and 74 cm (starting time March 25, 00:00)*

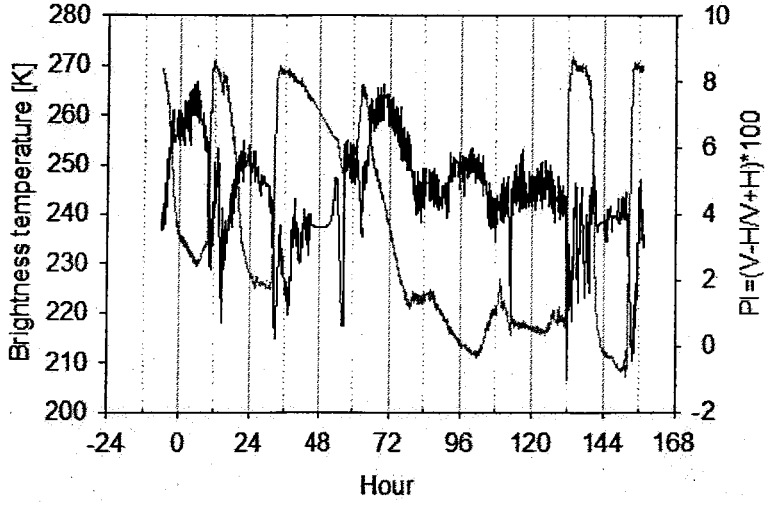

Figure 5 *Polarization index at 37 GHz as a function of time. Brightness temperature at 37 GHz V pol. Is reported as a reference for melting-refreezing cycles*

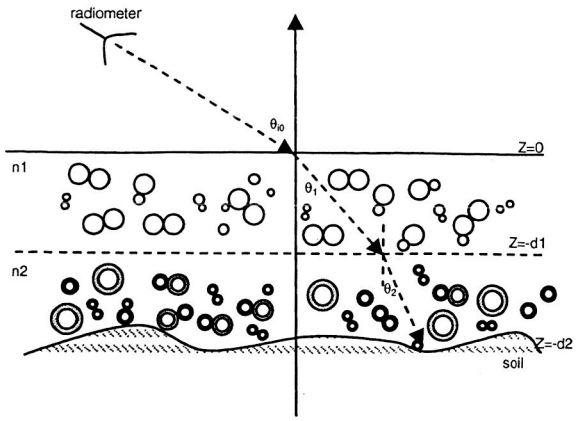

Figure 6 Representation of the snowpack used in the DMRT

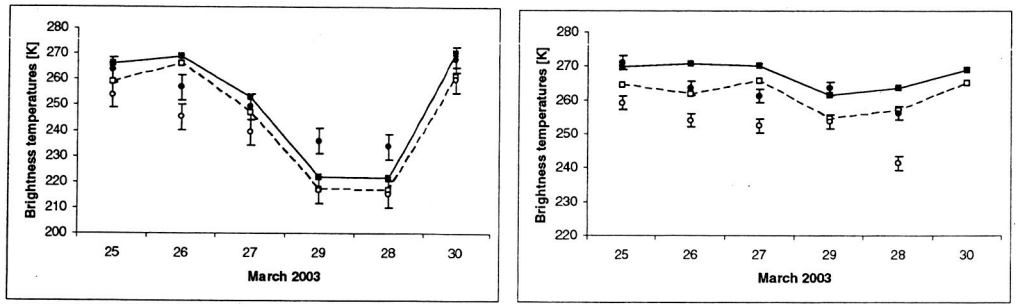

19 GHz 37 GHz

Figure 7

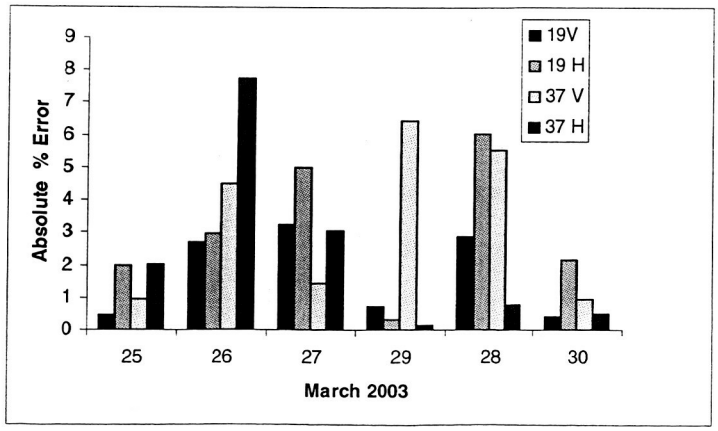

Figure 8

DATE (SNOW PIT)	THICKNESS [M]	DENSITY [KG/M3]	TEMP. [K]	WETNESS [%]

	Lyr 1	Lyr 2	Lyr1	Lyr2	Lyr1	Lyr2	Lyr1	Lyr2
03/25 (4A)	0.15	0.40	230	250	272	273.15	0	0.5
03/26 (3A)	0.1	0.71	195	306	273.15	273.15	0.3	0.7
03/27 (4B)	0.35	0.30	190	277	272.5	273.15	0.06	1
03/28(3C)	0.4	0.45	223	331	269.2	273.15	0	0.2
03/29 (4C)	0.20	0.4	225	294	270	273.15	0	0.6
03/30 (3C)	0.1	0.77	214	301	273.15	273.15	1.3	1.5

Table 1 Inputs to the electromagnetic models obtained from snow pit data

DATE (SNOW PIT)	AVG. SM, MD, LG SHORT / LONG AXIS		AVG. MD,LG SHORT / LONG AXIS		ONLY LG SHORT / LONG AXIS	
	Lyr1	Lyr2	Lyr1	Lyr2	Lyr1	Lyr2
03/25 (4A)	0.41/0.42	0.51/0.66	0.51/0.5	0.6/0.77	0.56/0.66	0.65/1
03/26 (3A)	0.5/0.6	1.13/1.33	0.6/0.7	1.35/1.65	0.6/1	2/2.3
03/27 (4B)	0.51/0.6	1.1/1.23	0.68/0.81	1.3/1.5	0.81/1.07	1.6/2
03/28(3C)	0.29/0.33	1.1/1.64	0.38/0.45	1.31/2.05	0.54/0.58	1.65/2.45
03/29 (4C)	0.5/0.68	1.14/1.4	0.61/0.86	1.48/1.88	0.7/1.16	1.7/2.5
03/30 (3C)	0.26/0.3	1.6/2	0.35/0.4	2/2.5	0.5/0.5	2.5/3

Table 2 Weighted averages of mean particle size using the values of the Small, Medium and Large classes (left), only the values of the Medium and Large (centre) and only the values of the class Large